Title

The kinases PIG-1 and PAR-1 act in redundant pathways to regulate asymmetric division in the EMS blastomere of C. elegans

Journal

Developmental Biology, 444(1)

ISSN

0012-1606

Authors

Liro, Małgorzata J
Morton, Diane G
Rose, Lesilee S

Publication Date

2018-12-01

DOI

10.1016/j.ydbio.2018.08.016

Peer reviewed

HHS Public Access

Author manuscript

Dev Biol. Author manuscript; available in PMC 2019 December 01.

Published in final edited form as:

Dev Biol. 2018 December 01; 444(1): 9–19. doi:10.1016/j.ydbio.2018.08.016.

The kinases PIG-1 and PAR-1 act in redundant pathways to regulate asymmetric division in the EMS blastomere of *C. elegans*

Małgorzata J. Liro[#a,*], **Diane G. Morton**[#b], and **Lesilee S. Rose**[a]

[a]Department of Molecular and Cellular Biology and Graduate Program in Biochemistry, Molecular, Cellular and Developmental Biology, University of California, Davis, CA, 95616

[b]Department of Molecular Biology and Genetics, Cornell University, Ithaca NY 14853

[#] These authors contributed equally to this work.

Abstract

The PAR-1 kinase of *C. elegans* is localized to the posterior of the one-cell embryo and its mutations affect asymmetric spindle placement and partitioning of cytoplasmic components in the first cell cycle. However, *par-1* mutations do not cause failure to restrict the anterior PAR polarity complex to the same extent as mutations in the posteriorly localized PAR-2 protein. Further, it has been difficult to examine the role of PAR-1 in subsequent divisions due to the early defects in *par-1* mutant embryos. Here we show that the PIG-1 kinase acts redundantly with PAR-1 to restrict the anterior PAR-3 protein for normal polarity in the one-cell embryo. By using a temperature sensitive allele of *par-1,* that exhibits enhanced lethality when combined with a *pig-1* mutation, we have further explored roles for these genes in subsequent divisions. We find that both PIG-1 and PAR-1 regulate spindle orientation in the EMS blastomere of the four-cell stage embryo to ensure that it undergoes an asymmetric division. In this cell, PIG-1 and PAR-1 act in parallel pathways for spindle positioning, PIG-1 in the MES-1/SRC-1 pathway and PAR-1 in the Wnt pathway.

Keywords

pig-1; *par-1*; let-99; spindle orientation; asymmetric division; endoderm specification

Introduction

Asymmetric divisions are important for cell fate diversity during development and for stem cell maintenance. In the process of asymmetric cell division, cell fate determinants become asymmetrically distributed along an axis of polarity. Concurrently, the mitotic spindle aligns along the polarity axis and signals the cleavage plane to bisect the determinant asymmetry,

[*]Address correspondence to Lesilee S. Rose, lsrose@ucdavis.edu, Dept. of MCB, One Shields Ave, University of California Davis CA 95616, Phone: 530-754-9884; Fax: 530-752-3085.

ultimately producing two differentially fated daughter cells. Incorrect distribution of cell fate determinants as a result of mitotic spindle misorientation has been linked to changes in cellular proliferation, cell fate specification and cancer (Bergstralh et al., 2017; Neumuller and Knoblich, 2009).

The *Caenorhabditis elegans* one-cell embryo is a classical model system for studying the process of asymmetric cell division. The sperm entry point marks the posterior end of the embryo and the sperm centrosomes are required for initiating symmetry breaking, which then leads to the establishment of anterior-posterior polarity. During symmetry breaking a cortical actomyosin network, containing the non-muscle myosin II heavy chain NMY-2, flows away from sperm and associated centrosomes. The posterior, non-contractile cortex expands towards the anterior until it reaches about 50% embryo length, and a prominent pseudocleavage furrow is present at the border of the contractile and non-contractile domains. These contractility differences along the one-cell cortex occur concurrently, and are partially required for, the asymmetric segregation of PAR proteins (Rose and Gonczy, 2014; Wu and Griffin, 2017).

PAR polarity proteins were named after their mutant phenotype; failure of asymmetric *par*titioning of cytoplasmic components, including cell fate determinants in the one-cell embryo, results in altered cell fate, cell size, cell cycle timing and often abnormal spindle positioning, which leads to catastrophic defects in developmental patterning (Kemphues et al., 1988). Several of the PAR polarity proteins are polarized along the anterior-posterior (AP) axis during polarity establishment. The PDZ-containing proteins PAR-3 and PAR-6 and the atypical protein kinase C, PKC-3, initially localize around the entire cell cortex. These “anterior” PARs then become localized to the anterior domain in an NMY-2 dependent fashion, allowing PAR-2, a RING-finger protein and PAR-1, a Serine/Threonine kinase, to localize to the reciprocal posterior domain of the embryo (Goldstein and Macara, 2007; Rose and Gonczy, 2014; Wu and Griffin, 2017). Following establishment of these domains, PAR proteins mutually exclude each other from their distinct anterior and posterior domains to maintain cell polarity. PAR proteins are required for posterior localization of the cell fate determinant PIE-1 (Tenenhaus et al., 1998) and germ-line P granules (Kemphues et al., 1988) as well as for anterior segregation of somatic precursor cell fate determinants such as MEX-5 (Schubert et al., 2000). The distinct PAR domains are also important for regulating other cortical proteins that control the alignment of spindle with cell fate determinants to ensure generation of properly fated daughter cells following cell division (di Pietro et al., 2016; Rose and Gonczy, 2014).

The *par-1* gene was initially identified in a screen for maternal effect lethal mutations that disrupt asymmetric spindle placement and partitioning of cytoplasmic components in the one-cell embryo (Kemphues et al., 1988). *par-1* mutants have a more symmetric first cleavage and synchronous cell cycles at the two-cell stage, similar to that observed in *par-2* mutants. At the same time, the effect of *par-1* mutations on maintenance of the PAR polarity domains and spindle orientation at the two-cell stage is much weaker than that of *par-2*, raising the possibility that another protein functions redundantly with PAR-1 in these processes (Cuenca et al., 2003; Etemad-Moghadam et al., 1995; Kemphues et al., 1988).

Morton and colleagues identified a set of genes that when knocked down by RNA interference (RNAi) do not cause much embryo lethality on their own, but cause higher embryo lethality when combined with the *par-1(zu310ts)* temperature-sensitive mutation at semipermissive temperature (Morton et al., 2012). One of these genes was *pig-1*, which encodes a serine/threonine kinase orthologous to vertebrate Maternal Embryonic Leucine zipper Kinase (MELK) and related to the PAR-1 kinase. PIG-1 was originally described for its role in regulating cell size and cell fate during asymmetric division of neuroblasts, in the late embryo and L1 larva (Cordes et al., 2006; Wei et al., 2017). *pig-1(RNAi)* also enhanced the lethality of *par-2(it5ts*) embryos at semi-permissive temperature and *pig-1(RNAi); par-2(it5ts)* embryos showed greater defects in maintaining the anterior PAR domain boundary in the one-cell embryo and stronger defects in two-cell asymmetries compared to *par-2(it5ts)* alone (Morton et al., 2012). These observations indicate that PIG-1 plays a role in early polarity, but neither the *pig-1* early embryonic phenotype nor its potential redundancy with *par-1* in the one-cell embryo have been analyzed in detail.

PAR domains are re-established in the posterior P_1 cell after the first division, and P_1 then divides asymmetrically to produce another germ-line precursor, P_2, and the endomesodermal precursor cell, EMS. The EMS cell divides asymmetrically to produce the anterior MS daughter cell, which primarily produces mesodermal cells, and the smaller posterior daughter cell, E, which gives rise to the entire endoderm of the worm. The EMS division orientation is due to a 90° rotation of the nuclear-centrosome complex that occurs prior to nuclear envelope breakdown (NEB) such that spindle forms on the cell's AP axis. Blastomere isolation and reconstitution experiments showed that both the division orientation and the fate asymmetry of the EMS daughter cells depend on a signal from the P_2 cell (Goldstein, 1993, 1995a, b; Maduro, 2017; Rose and Gonczy, 2014). Subsequent genetic screens for mutants producing more mesoderm at the expense of endoderm tissue ("*mom*" mutants) identified several components of the Wnt signaling pathway as being partially required for endoderm specification. A subset of Wnt signaling components, such as the Wnt ligand (MOM-2 in *C. elegans*), the Frizzled receptor (MOM-5), and the Disheveled adaptor proteins (DSH-2 and MIG-5) are also required for timely spindle orientation. Embryos mutant for these components can exhibit a failure of nuclear rotation by NEB, but most embryos eventually orient their spindles onto the AP axis in anaphase (Bei et al., 2002; Liro and Rose, 2016; Schlesinger et al., 1999). A similar late EMS spindle rotation phenotype is exhibited by mutants in the MES-1/SRC-1 pathway (Bei et al., 2002). However, when embryos are mutant for components in both the Wnt and MES-1/SRC-1 pathways, EMS spindle positioning fails completely in most embryos, resulting in divisions along the left-right (LR) axis (Bei et al., 2002). Although *mes-1* and *src-1* single mutants do not have defects in endoderm fate specification, double mutants with Wnt pathway components produce a higher frequency of failure to specify endoderm than in *wnt* single mutants. Thus, the MES-1/SRC-1 pathway acts in parallel to the Wnt pathway for both EMS spindle orientation and endodermal specification (Bei et al., 2002).

The MES-1/SRC-1 pathway has only a few known components. SRC-1, a tyrosine kinase, and MES-1, a transmembrane receptor tyrosine kinase-like protein, both localize to the cell-cell interface between P_2 and EMS (Bei et al., 2002; Berkowitz and Strome, 2000). NMY-2 was shown to be upstream of SRC-1 for endoderm specification, but not spindle positioning

(Liu et al., 2010). Recently, LET-99, a protein required for spindle positioning in the one-cell embryo (Krueger et al., 2010; Park and Rose, 2008; Rose and Kemphues, 1998; Tsou et al., 2002; Wu and Rose, 2007), was shown to play a role in EMS spindle positioning downstream of the MES-1/SRC-1 signal (Bei et al., 2002; Liro and Rose, 2016). In the one-cell embryo, LET-99 is asymmetrically localized at the cortex in response to the PAR proteins, where it then acts to localize the force generation complex that aligns the spindle on the PAR polarity axis. However, in the EMS cell, the PAR domains localize to distinct inner and outer domains (Nance and Priess, 2002), and thus are not aligned with the AP axis and the spindle as they are in the one-cell. Whether *par* genes are required during EMS asymmetric division has not been assessed, due to their mutant phenotypes prior to this stage.

Here, we further investigate the roles of PIG-1 in the *C. elegans* embryo and how PIG-1 may be synergizing with PAR-1. We find that PIG-1 acts in parallel with PAR-1 in regulating restriction of the anterior polarity complex at the one-cell stage. We further find that PIG-1 acts to regulate EMS spindle orientation in the MES-1/SRC-1 pathway, and PAR-1 acts in the parallel Wnt pathway. Moreover, in addition to its role in spindle positioning, PIG-1 appears to play a role in endoderm cell fate specification.

Results

PIG-1 acts with PAR-1 to restrict the anterior PAR domain in the one-cell *C. elegans* embryo.

Worms homozygous for the *pig-1(gm344)* null mutation (Cordes et al., 2006) are approximately 9% embryonic lethal and 15% larval lethal, at 19.5°C (Table S1). Thus, the *pig-1* gene, while not essential for viability, makes a clearly discernable contribution to development. We compared viability at different temperatures, and found that at a higher temperature of 25°C, embryo lethality was increased to 14% in *pig-1(gm344)* mutants (hereafter referred to as *pig-1* mutants; Table S1). The terminal phenotypes of the dead embryos showed that they had many differentiated cell types, but lacked morphogenesis. This phenotype has also been observed in embryos produced by mothers homozygous for maternal effect lethal mutations in the *par* genes (Kemphues et al., 1988). In addition, *pig-1(RNAi)* was previously found to enhance the lethality of *par-1* and *par-2* temperature-sensitive mutants (Morton et al., 2012). Given the structural similarities between PIG-1 and PAR-1 kinases, we examined early polarity of *pig-1* mutants alone and in combination with the *par-1(zu310ts)* temperature-sensitive mutation (referred to hereafter as *par-1(ts)* for simplicity), using time-lapse microscopy. Mothers homozygous for the *par-1(ts)* allele grown at 25°C produce embryos with a strong *par-1* phenotype, but very few defects are observed when worms are grown at the semi-permissive temperature of 19.5 °C (Table S1, see also Material and Methods (Morton et al., 2012; Spilker et al., 2009)).

Before pronuclear meeting in the newly-fertilized wild-type embryo, a series of myosindriven contractions facilitates a rearrangement of the cortex and allows polarization of cortical PAR proteins into their anterior and posterior domains. A signature of this reorganization is the presence of anterior cortical contractions that resolve into a single pseudocleavage furrow at midembryo length, which then relaxes after pronuclear meeting

(Fig. 1A and Movie S1). Time-lapse imaging revealed that *pig-1* embryos grown at either 19.5°C or 25°C exhibited a reduction in anterior cortical ruffling and formation of the pseudocleavage furrow (Fig. 1A and Movie S2). Quantification of embryos at 25**x**C confirmed that the extent of pseudocleavage furrow ingression was reduced to 12% embryo width (% EW) in *pig-1* embryos (N=10), as compared to 46% EW in control embryos. The furrow was also positioned more posteriorly in *pig-1* embryos at 58% embryo length (% EL) in *pig-1* embryos, as compared to 48% EL in controls (N=12) (Fig. 1B, C). In *par-1(ts)* single mutants grown at 25°C (N=13), a weaker (23%EW) more anteriorly positioned pseudocleavage furrow (44% EL) was observed, as reported previously for other *par-1* mutants (Cuenca et al., 2003; Kirby et al., 1990). In *pig-1; par-1(ts)* double mutants (N=11), the position of the pseudocleavage furrow (51% EL) was restored to that of controls. On the other hand, the extent of ingression of the pseudocleavage furrow was greatly reduced to 7% EW in *pig-1; par-1(ts)* double mutants, as seen for *pig-1* single mutants (Fig. 1A, B, C; specific comparisons are highlighted, all p values can be found in Table S2).

The abnormalities in cortical contractility exhibited by *pig-1* embryos suggested that there might also be defects in PAR domain establishment or maintenance. In addition, previous work showed that although *par-1* mutant zygotes have a distinct anterior PAR-3 domain, the extent of the domain expands slightly towards the posterior during the maintenance phase in *par-1(RNAi*) one-cell embryos (Cuenca et al., 2003). These observations suggest that PAR-1 may participate in restriction of the anterior polarity complex but perhaps redundantly with another protein. We therefore examined PAR-3 localization in *pig-1* single mutants and in combination with *par-1(RNAi)* and the *par-1(ts*) mutation at 25°C. In wild-type embryos, the anterior PAR-3 domain extended to 51.6% EL. We found that in *pig-1* mutants, the anterior PAR-3 domain extended slightly further into the posterior during anaphase, to 57.4% EL, similar to the PAR-3 domain in *par-1(ts)* embryos (55.8% EL) and *par-1(RNAi)* embryos (63.2 % EL) (Fig. 1E, F). Examination of the PAR-3 domain in *pig-1; par-1(ts)* double mutant embryos as well as in *pig-1; par-1(RNAi)* embryos revealed an even greater expansion of the PAR-3 domain (to 71.4% and 86.1% EL, respectively; Fig. 1E, F). Thus, *pig-1* and *par-1* act redundantly to restrict the size of the anterior PAR-3 domain at the one-cell stage.

Despite the changes in the one-cell described above, first cleavage anaphase spindles were aligned with the AP axis and displaced towards the posterior in *pig-1* embryos (N=10), as in control embryos (N=12) (Fig. 1A). Moreover, as reported previously the first mitotic division in *pig-1* embryos was unequal (Pacquelet et al., 2015), producing AB and P_1 daughter cells of different sizes. The position of the boundary between AB and P_1 at early interphase was 61% EL (N=13), similar to controls (59% EL, N=9) (Fig. 1D). The first division was also oriented normally and unequal in *par-1(ts)* mutants (44%EL, N = 12) as well as in *pig-1; par-1(ts)* double mutant embryos ((51 %EL), N= 12).

PIG-1 and PAR-1 are required for spindle orientation in the EMS cell

In addition to the enhancement of one-cell polarity defects observed at 25°C, *pig-1; par-1(ts)* mutants raised at the semi-permissive temperature of 19.5°C exhibited a high level of embryonic lethality (68%) compared to *pig-1* and *par-1(ts)* single mutants (9% and 5%

respectively, Table S1). This is similar to the previously reported enhancement of *par-1(ts)* by *pig-1(RNAi),* observed at 19°C (Morton et al., 2012). However, in that study, it was found that P granules localized normally and second division spindle orientation was unaffected in *pig-1(RNAi); par-1(ts*) two-cell embryos (Morton et al., 2012). We therefore set out to determine if other aspects of early embryonic development are affected in *pig-1* and *pig-1;par-1(ts)* embryos. Because our analysis of the *par-1(ts)* allele revealed that it is a slow-inactivating temperaturesensitive allele (see Material and Methods), mutants were grown and imaged at the semipermissive temperature of 19.5 °C.

First we examined the cell cycle at second and third division, since wild-type embryos exhibit characteristic differences in cleavage timing that are dependent on normal PAR function. At second cleavage, the anterior AB cell divides before the P_1 cell (126 sec on average, Fig. 2A, B). At third cleavage, the AB daughter cells divide synchronously, followed by the EMS cell, which divides before the P_2 cell (232 sec on average). Compared to wild type, *par-1(ts)* single mutants, grown and filmed at semi-permissive temperature, exhibited more synchronous cell cycles (43 sec for AB-P_1 and 112 sec for EMS-P_2), as expected for *par-1* mutants (Kemphues et al., 1988; Spilker et al., 2009) (Fig. 2B, 2B). Examination of *pig-1* mutant embryos revealed that the AB and P_1 daughter cells also divided with more similar cell cycle rates than in wild type (96 sec on average; Fig. 2A, B). However, at the third division, the difference between the EMS and P_2 cell cycles of *pig-1* mutants (214 sec on average) was not statistically different from wild type. The AB-P_1 and EMS-P_2 cell cycles of *par-1(ts);pig-1* double mutants were also more synchronous than controls, but were not significantly different than those of *par-1* alone.

As another readout of early polarity, we characterized P_1 and EMS spindle positioning. In wild-type embryos at second cleavage, the P_1 nucleus exhibits a nuclear rotation event so that the spindle forms on the AP axis once again. At the four-cell stage, the nucleus in EMS also rotates onto the AP axis, prior to nuclear envelope breakdown (Fig. 2A). In contrast to the cell cycle abnormalities observed at the two-cell stage, both *par-1(ts)* (N= 10) and *pig-1* mutants (N = 10) exhibited normal P_1 rotation onto the AP axis, just as in wild type (Fig. 2A, B and see below). Similarly, *pig-1; par-1(ts)* double mutants showed normal P_1 spindle orientation at the two-cell stage (N =12). However, at the four-cell stage, the EMS spindle of the *pig-1; par-1(ts)* double mutants was misoriented. We found that less than half of *pig-1; par-1(ts)* embryos imaged at 19.5°C exhibited a normal EMS nuclear-centrosome rotation prior to nuclear envelope breakdown. Instead, 53% of *pig-1; par-1(ts)* embryos completely failed rotation and thus their EMS spindles were oriented on the LR axis or on an oblique axis (Fig. 2C, N=32). In comparison, single *pig-1* or *par-1(ts)* mutants imaged at 19.5°C showed only a low level of late spindle alignment or LR divisions (Fig. 2C, N= 17 and 27). In embryos raised and filmed at the nonpermissive temperature of 25°C, P_1 division orientation was still normal in *pig-1; par-1(ts)* double mutants (N=8); however, the frequency of LR division defects in EMS was 100%, as seen for *par-1(ts)* alone (N=8, 9). Together these observations reveal that there is redundancy between *par-1* and *pig-1* for EMS division orientation, but not for P_1 division orientation.

Since the P_2 blastomere signals to EMS to guide its spindle positioning and cell fate specification, we examined *pig-1; par-1(ts)* double mutants for defects in cell fate

specification at the four-cell stage. P granules, a germ-line marker, are segregated to the P_1 cell and the P_2 cell in a PAR dependent manner during the first divisions of wild-type embryos (Kemphues et al., 1988; Strome and Wood, 1982). We found that in *pig-1* and *par-1(ts)* single and double mutants raised at 19.5°C, P granules were normally localized at 2- and 4-cell stages (N=4, N=30, N=6, respectively) as in wild-type controls (N=15). PIE-1 is a determinant of germ line fate that is also enriched in the posterior P blastomeres at each of the early divisions (Mello et al., 1996). PIE-1 was normally localized in two and four-cell embryos of *pig-1; par-1(ts)* double mutants (N=11), as in wild type (N=27), at 19.5°C (Fig. 3A). These data suggest that at least some aspects of the P_1 asymmetric division and subsequent fate of P_2 are preserved in *pig-1; par-1(ts)* double mutants at the semi-permissive temperature.

To directly assay the ability of P_2 to signal to EMS at the four-cell stage, we examined activation of SRC-1 using immunostaining with the pY99 monoclonal antibody that recognizes phosphotyrosine. Previous work showed that wild-type embryos exhibit a relative enrichment of the pY99 signal at the P_2/EMS interface compared to other cell-cell contacts; the pY99 signal is uniform in *mes-1* mutants and is abolished in *src-1* mutants (Bei et al., 2002). To quantify cortical enrichment of pY99 at the P_2/EMS interface, we measured the average pixel intensities at the P_2/EMS and ABp/EMS interfaces. In wild-type embryos, pY99 staining was enriched, approximately 2.3 fold, at the P_2/EMS contact site compared to the ABp/EMS interface. This enrichment was abolished in *mes-1* mutants (Fig. 3B, 3C). In *pig-1* and *par-1(ts)* single mutants at the semi-permissive temperature, enrichment was also evident at the P_2/EMS contact. Although the average enrichment was lower than in wild type, 100% of *par-1(ts)*, and 85% of *pig-1* embryos showed pY99 enrichment that fell within the wild-type range, compared to 0% of *mes-1* embryos (Fig. 3C). Thus, the majority of single mutant *pig-1* or *par-1(ts)* embryos appear to have intact MES-1/SRC-1 signaling. The enrichment observed in *pig-1; par-1(ts)* double mutants was on average lower than either single mutant; nonetheless, 79% of those embryos had some pY99 enrichment at the P_2/EMS contact site compared to the ABp/EMS contact site (cortical ratio greater than 1.0) and the enrichment was within the wild-type range in 58% of embryos (Fig. 3C). Together, the P granule, PIE-1 and the pY99 localization data suggest that many aspects of P_2 and EMS cell fate are normal in the single *par-1(ts*) and *pig-1* mutants at the semi-permissive temperature. The *pig-1; par-1(ts)* double mutant however, does show a small but significant reduction in pY99 signal between P_2 and EMS compared to the single mutants. MES-1 was previously shown to be completely absent in a strong *par-1* mutant (Berkowitz and Strome, 2000). Thus, our observations of reduced pY99 signal in the *pig-1; par-1(ts)* double mutant are consistent with PIG-1 and PAR-1 being partially redundant for proper MES-1/SRC-1 signaling.

PIG-1 acts in the MES-1/SRC-1 pathway for EMS spindle positioning and endoderm specification.

The EMS spindle positioning defects observed in the *pig-1* mutant are reminiscent of mutants in the Wnt or MES-1/SRC-1 pathways, which exhibit a low frequency of failed or late EMS spindle rotations (Bei et al., 2002; Liro and Rose, 2016; Schlesinger et al., 1999). Double mutants of components in the same pathway do not show any enhancement of

spindle positioning defects, as compared to single mutants alone. In contrast, the majority of *wnt; mes-1* double mutants exhibit a complete failure of EMS nuclear/spindle rotation so that the spindle remains on the LR or other non-AP axis. We therefore imaged *pig-1* embryos in combination with depletion of Wnt or MES-1/SRC-1 pathway components via RNAi to determine if PIG-1 acts in either pathway. The EMS spindle positioning defects of *pig-1* embryos were enhanced by RNAi of the Wnt components *mom-2* (the ortholog of the vertebrate Wnt ligand) and *dsh-2;mig-5* (vertebrate Dsh orthologs), to 69% and 73%, respectively (Fig. 4A). EMS spindle orientation defects seen in *pig-1; wnt(RNAi)* double mutants were comparable to those seen in *mes-1; wnt(RNAi)* embryos. However, *mes-1(RNAi)* did not enhance *pig-1* single mutant EMS spindle positioning defects (Fig. 4A). These results are consistent with PIG-1 acting in the MES-1/SRC-1 pathway for spindle orientation.

We previously found that LET-99 also acts in the MES-1/SRC-1 pathway for spindle positioning (Liro and Rose, 2016). Upshift of embryos from mothers homozygous for the temperature sensitive *let-99(ax218ts)* mutation at the early four-cell stage did not result in strong spindle positioning defects, and did not cause a significant change in the weak spindle positioning defects exhibited by *mes-1(RNAi)* embryos. However, the *let-99(ax218ts)* mutation did suppress the stronger spindle positioning defects of *src-1* mutants and *mes-1(RNAi);mom-2(RNAi)* double mutants (Liro and Rose, 2016). We therefore examined EMS spindle positioning in *pig-1; let-99(ax218ts)* and *pig-1; let-99(ax218ts); mom-2(RNAi)* embryos upshifted at the four-cell stage. Spindle positioning defects were reduced in *pig-1; let-99(ax218); mom-2(RNAi)* embryos compared to *pig-1;mom-2(RNAi)* embryos (24% versus 69%; Fig. 4B). This suppression suggests that LET-99 acts downstream of PIG-1 in the MES-1/SRC-1 pathway.

To determine if PIG-1 also plays a role specifying endoderm fate in the MES-1/SRC-1 pathway, we examined embryos for the presence of gut cells, which are derived from the E daughter of EMS. Single *mes-1* mutants do not have defects in endoderm specification, and many *wnt* mutants display a low frequency of the endoderm specification, or gutless, phenotype. However, as with spindle positioning, endoderm defects are enhanced in *wnt; mes-1* double mutants (Bei et al., 2002). Embryos were examined for the presence of autofluorescent gut granules, a marker of gut cells, at a time when control embryos had hatched into larvae (Laufer et al., 1980). As previously reported, only a small fraction of control embryos treated with *mom-2(RNAi),* or *dsh-2(RNAi);mig-5(RNAi)* failed to produce gut granules, 1% and 15% respectively (Fig. 5A). While all *pig-1* single mutant late-stage embryos had gut granules, *pig-1; mom-2(RNAi)* and *pig-1; dsh-2(RNAi); mig-5(RNAi)* exhibited a gutless phenotype at a high frequency of 57%, which is similar to that seen in *mes-1; mom-2(RNAi)* (53%) and *mes-1; dsh-2(RNAi);mig-5(RNAi)* (50%) double mutants. In contrast, none of the *pig-1; mes-1(RNAi)* embryos exhibited a gutless phenotype (Fig. 5B). Thus, *pig-1* enhances the gutless phenotype of Wnt pathway mutants, but not of *mes-1* mutants. Together, these results suggest that PIG-1 acts in the MES-1/SRC-1 pathway for endoderm cell fate specification.

PAR-1 acts in the Wnt pathway for EMS spindle positioning

Previously characterized strong *par −1* loss-of-function mutations show a complete loss of endoderm (Kemphues et al., 1988). At the non-permissive temperature of 25°C, *par-1(ts)* single mutants showed a strong reduction in endoderm specification (80% gutless, N=35). The cell fate specification phenotype was enhanced to 100% gutless in *pig-1; par-1(ts)* double mutant embryos at 25°C (N= 21). Given PAR-1's role in early divisions and cytoplasmic asymmetry, the endoderm specification and spindle positioning defects observed are likely due, at least in part, to abnormalities in P_2 cell fate that may abrogate both Wnt and MES-1/SRC-1 signaling.

Because *par-1(ts)* is a slow-inactivating allele, we were unable to perform temperature upshift experiments to test its role more specifically in the EMS division. Instead, we again examined *par-1(ts)* at the semi-permissive temperature of 19.5°C, in combination with RNAi of Wnt or MES-1/SRC-1 pathway components. The EMS spindle positioning defects of *par-1(ts)* embryos at 19.5°C were enhanced to 80% when combined with *mes-1*(RNAi), but no enhancement was observed with *mom-2 (RNAi)* (Fig. 4C). Neither *wnt* nor *mes-1* RNAi treated *par-1(ts)* embryos showed enhancement of the gutless phenotype at the semi-permissive temperature (Fig. 5B). However, *pig-1; par-1(ts)* embryos did exhibit a strong gutless phenotype at 19.5°C (Fig. 5A). These data are consistent with PAR-1 acting in the Wnt pathway, in parallel to the MES-1/SRC-1 pathway, for at least EMS spindle positioning.

Discussion

While PIG-1 was first characterized for its role in governing neuroblast asymmetric divisions in the late embryo and L1 larva (Cordes et al., 2006; Wei et al., 2017), this study demonstrates an earlier role for PIG-1 during the very first embryonic asymmetric divisions. Overall, the phenotypes exhibited for *pig-1* single mutant embryos are less severe than those observed for most *par* mutant embryos, but nevertheless show that PIG-1 is important for some of the normal asymmetries of the early blastomeres. We provide insight into the role of PIG-1 in regulating the domains of the conserved and well-studied PAR proteins, and reveal that PIG-1 plays a role in another asymmetric cell division, that of the EMS blastomere.

PAR polarity proteins need to be localized to distinct anterior versus posterior domains for successful asymmetric division of the *C. elegans* one-cell embryo, and multiple mechanisms ensure that polarity is established and maintained prior to division. The first mechanism for establishment involves an unknown cue from the sperm centrosome that causes actomyosin flow towards the opposite end of the embryo, the anterior end; this results in concomitant movement of PAR-3, PAR-6 and PKC-3 to the anterior (Munro et al., 2004), and it is stabilized by feedback between clustered PAR protein complexes (Sailer et al., 2015). In a secondary mechanism, the microtubules nucleating from the sperm centrosome mediate posterior cortical PAR-2 association, which then recruits PAR-1; PAR-1 phosphorylates PAR-3, preventing it from associating with the posterior domain (Motegi et al., 2011; Zonies et al., 2010). Polarization kinetics are slower when one of those mechanisms is compromised. Further, although an anterior PAR domain can be established in the absence of PAR-2, PAR-2 is essential during the maintenance phase to prevent anterior PARs and NMY-2 from invading the posterior domain. In contrast, *par-1* mutants have weaker polarity

defects (Cheeks et al., 2004; Cuenca et al., 2003; Kirby et al., 1990; Small and Dawes, 2017). Cortical flow and the establishment of the anterior and posterior PAR domains appear normal in *par-1(RNAi)* and *par-1* mutants, although pseudocleavage and the initial boundary between PAR domains are often more anteriorly positioned than in wild type. During maintenance, there is only a slight expansion of the anterior PARs towards the posterior in *par1(RNAi)* embryos, and by the two-cell stage PAR domains are again normal (Cuenca et al., 2003). Further, NMY-2::GFP levels are not altered in *par-1* mutants, and NMY-2 does not flow back into the posterior (Small and Dawes, 2017). Our observations revealed that *pig-1* mutants have greatly reduced cortical contractility in early one-cell embryos, suggesting a defect in NMY-2 mediated polarity establishment. Thus, the enhanced expansion of the anterior PAR domain in *pig-1; par-1* double mutants could be explained by reduced NMY-2 activity in the *pig-1* mutant during establishment, combined with reduced PAR-1 activity in the PAR-2 pathway during either establishment or maintenance. It was recently shown that PAR-3 may be a target of the PIG-1 kinase (Offenburger et al., 2017); PAR-3 is known to regulate myosin activity in a positive feedback loop at pseudocleavage (Munro et al., 2004). Therefore, PIG-1 might indirectly regulate myosin at the pseudocleavage stage via PAR-3. Surprisingly, a recent study concluded that PIG-1 inhibits cortical accumulation of activated myosin, rather than promotes it, during cytokinesis in the *C.elegans* one-cell (Pacquelet et al., 2015). These differing results suggest that PIG-1 may have opposite effects on actomyosin contractility in the same cell at different time points, likely by regulating different intermediates.

Our data also indicate that PIG-1 is required for both spindle positioning and endoderm fate specification in the EMS cell in the MES-1/SRC-1 pathway. NMY-2 has been placed in the MES-1/SRC-1 pathway for endoderm specification based on enhancement of the gutless phenotype of *wnt* mutants, however spindle orientation was not affected. Further, it was found that *nmy-2(ts)* mutants showed reduced enrichment of the phosphotyrosine marker for SRC-1 activation at the P_2/EMS boundary, suggesting that NMY-2 acts upstream of SRC-1 (Liu et al., 2010). In contrast, we found that the enrichment for pY99 was normal in the majority of *pig-1* single mutants, and *pig-1* enhanced both spindle positioning and endoderm specification defects of *wnt(RNAi)* embryos. Thus, PIG-1 likely acts downstream of SRC-1 in the EMS cell to promote its asymmetric division. Additionally, in early *C. elegans* embryos, PIG-1 was reported to localize in the cytoplasm and also at the cell cortex during mitosis (Pacquelet et al., 2015). The cortical localization of PIG-1 raises the possibility that PIG-1 may act with the cortically anchored spindle positioning machinery. At the same time, we cannot rule out an additional, partially redundant role for PIG-1 in the P_2 cell, given the reduction in pY99 staining exhibited by *pig-1; par-1(ts)* double mutants, at semi-permissive temperature, compared to *pig-1* or *par-1(ts)* single mutants. *par-1(ts)* mutant embryos at high temperature as well as other strong *par-1* mutants have a complete loss of endoderm (Kemphues et al., 1988); this could be due to defects in the first or second asymmetric division that result in a failure to localize determinants to the P_2 cell, or to a role in generating the MES-1 and Wnt signals at the 4-cell stage. Because the *par-1(ts)* allele is not fast-inactivating, we cannot distinguish between these possibilities.

In addition to specifying general P_2 fate, we speculate that PAR-1 may also play a more direct role in the Wnt pathway for EMS division. Our analysis of *par-1(ts)* mutants at the

semipermissive temperature showed that spindle positioning defects were enhanced by MES-1 depletion, but not a Wnt pathway component depletion. Similarly, *pig-1; par-1(ts)* embryos showed an enhancement of spindle positioning defects, consistent with PAR-1 and PIG-1 acting in parallel pathways to promote EMS spindle orientation. Surprisingly, we did not observe an enhancement of endoderm specification defects in *par-1(ts); mes-1* embryos at this temperature. It is possible that spindle positioning is more sensitive to the loss of *par-1* and *mes-1* than endoderm specification is. Alternatively, PAR-1 could act downstream of Wnt signaling in the EMS cell specifically to promote spindle positioning. Future studies identifying substrates of PAR-1 and PIG-1 will more fully elucidate their function in EMS cell fate specification and spindle orientation.

In summary, the PIG-1 protein, while not necessary for viability, clearly plays important roles to ensure robust early development in *C. elegans*. Our studies of the parallel requirements of *par-1* and *pig-1* show how important a “nonessential” kinase like PIG-1 is when a more essential effector, such as PAR-1, is weakly compromised. In this situation, roles for PIG-1 in regulating restriction of the anterior polarity protein PAR-3 in the zygote, control of cell division timing in the early embryo, and regulation of EMS spindle orientation and endoderm specification in *C. elegans* were revealed. Our analysis also showed that PAR-1 has a specific role in EMS cell division dynamics in a pathway separable from that of PIG-1. It would be interesting to test other potential PIG-1 kinase targets recently identified in a proteomic screen (Offenburger et al., 2017), for a role in regulating the fate and division orientation of the EMS blastomere. The mammalian homolog of PIG-1, MELK, is also nonessential for viability in mice ((Lin et al., 2017; Wang et al., 2014), but is highly expressed in mammalian embryonic cells, hematopoietic cells and neural progenitor cells (Gil et al., 1997; Heyer et al., 1997; Nakano et al., 2005). MELK is likely to act redundantly with other mitotic kinases, which may include closely related MARK family kinases, homologs of PAR-1 (Drewes et al., 1997). Our results also raise the possibility that mammalian MELK could participate in Src signaling pathways. Further characterization of PIG-1 genetic interactions and substrates in the *C. elegans* system should provide additional insights into the role of this conserved kinase in cell-cell signaling.

Materials and Methods

Worm strains and RNAi clones

C. elegans were grown on MYOB plates using standard conditions (Brenner, 1974; Church et al., 1995). Strains used were the following - N2: wild type, Bristol variant (Brenner, 1974); AZ244: *unc-119(ed3) III; ruIs57[pie-1::GFP::tubulin + unc-119(+)]* (Praitis et al., 2001); KK822: *par-1(zu310ts) V; KK863: sqt-3(sc8) par-1(zu310ts) V*; KK1083: *pig-1(gm344) IV* (outcrossed from NG4370: *zdIs5 I; pig-1(gm344)* (Cordes et al., 2006); KK1237: *pig-1(gm344) IV; sqt-3(sc8) par-1(zu310ts)* V; RL262: *mom-5(zu193) unc-13(e1091)/ hT2 I; +/hT2[bli-4(e937)let(h661)]; unc-119(ed3) III; ruIs57[pie-1::GFP::tubulin + unc-119(+)]*; RL292: *(bn7) X; unc-119(ed3)III; ruIs57[pie-1::GFP::tubulin + unc-119(+)]* (Liro and Rose, 2016); RL347: *pig-1(gm344) IV; ruIs57[pie-1::GFP::tubulin + unc-119(+)]*; RL355: *pig-1(gm344) let-99 (ax218) unc-30 (e1919) IV; ruIs57[pie-1::GFP::tubulin + unc-119(+)]*; SS392: *mes-1(bn74) X* (Berkowitz

and Strome, 2000). Temperature-sensitive strains were maintained at 16.0°C +/− 1.0°C and worms were shifted to 19.5 +/− 0.5°C or 25 +/− 0.5°C as L3/L4 for analyses. Other strains were maintained at 19.5 °C +/− 1.0°C.

RNAi was carried out by bacterial feeding (Timmons and Fire, 1998) using the following Ahringer library clones: *mes-1*(X-5L23), *mom-2* (V-6A13), *mig-5* (II-6C13), *dsh-2* (II-4011) (Kamath et al., 2003), and a *par-1* RNAi clone (Hurd and Kemphues, 2003). Worms were imaged 20–30hr post shift to 19.5°C.

Live imaging

Embryos were removed from gravid hermaphrodites and were mounted on 2% agarose pads on microscope slides and covered with coverslip. The initial time-lapse microscopy of embryos to compare cell cycle asynchrony was carried out using DIC optics on a Leica DM RA2 microscope with a Hamamatsu ORCAER digital camera or on an Olympus BX60 fitted with an Hamamatsu Orca C4742–95 camera, using Openlab or ImagePro software in a temperaturecontrolled room kept at (19.5°C). Subsequent analyses including combinations with RNAi were carried out using an Olympus BX60 microscope equipped with a Hammatasu Orca 12-bit digital camera and a Linkam PE95/T95 System Controller with an Eheim Water Circulation Pump to control specimen temperature; calibration of controller settings to true specimen temperature was carried out by inserting the wire probe of an Omega HH81 digital thermometer between the cover slip and an agar pad with the 60X objective and oil in place. The *par-1(zu310ts)* mutation was found to be a slow-inactivating temperature sensitive allele: Embryos from worms shifted from 16°C to 25°C for 18–24 hr showed synchronous cleavages and 100% abnormal orientation of the EMS cell division (N=9) regardless of imaging temperature. In contrast, embryos shifted from 16°C to 25°C for 10 min up to 100 min (N=8) appeared the same as those grown and imaged at 16°C. Thus for most experiments, the Linkam Controller was set to maintain a constant slide temperature of 19 +/− 0.5 °C or 25 +/− 0.5 °C to match growth conditions. For experiments using *let-99(ax218ts)*, embryos were imaged at 16.4–17.4°C to ensure proper P_1 spindle positioning and then upshifted to the non-permissive temperature of 25°C at the four-cell stage (at NEB of ABa and ABp) to examine EMS spindle positioning, as in (Liro and Rose, 2016). Single-plane images in brightfield optics were acquired every 10 sec using Micromanager 1.4.22.

Phenotypic analysis of live embryos

The extent and position of pseudocleavage were measured at maximum ingression, before pronuclear meeting. Using the Fiji line tool (Schindelin et al., 2012), the distance between opposing ingressing membranes and the distance of the widest part of the embryo in the same frame (embryo width, EW) were measured; the ratio of these two numbers was then subtracted from 1.0 to obtain the extent of ingression, expressed as %EW. The position of pseudocleavage was measured by drawing a straight line from the anterior most end of an embryo to the pseudocleavage furrow; embryo length (EL) was measured, and the ratio of pseudocleavage position to EL was taken to give %EL, where 0% is the anterior-most and 100% is the posteriormost point. The asymmetry of the first division was similarly measured by determining the %EL of the AB-P_1 cell-cell boundary at NEB of the AB cell cycle.

Spindle positioning in P cells was scored as normal if a line connecting the two centrosomes was within 30° of a line drawn along the anterior posterior axis; P_1 was scored just prior to NEB, while P_0 was scored at anaphase because both wild type and GFP::tubulin control embryos show variation at NEB. Cell cycle timing was examined by determining the difference between the time of NEB for AB versus P_1, or for EMS versus P_2. Statistical tests of significance were made using the Student's t-test in Excel and graphs were made using GraphPad Prism Version 6.0. EMS spindle positions were categorized as in Liro and Rose (2016): AP, spindle initially formed on the AP axis (aligned before NEB); late, spindle formed on the LR, dorsal-ventral (DV) or other non-AP axis and then rotated onto the AP axis; LR/DV, the spindle formed on a non-AP axis and never rotated. EMS phenotypes were grouped as normal (AP) or abnormal (late or LR/DV) and compared using Chisquared analysis in Excel. Graphs were made in GraphPad Prism Version 6.0.

Analysis of gut cell fate specification

Gut cell differentiation was scored in the same embryos filmed for the spindle positioning data or in embryos from siblings worms raised in parallel and mounted on agar pads. Slides were incubated in a moist chamber until the time that normal embryos would hatch (at least 12 hours at 25°C or 24 hours at 19.5 °C). UV light or polarization optics were used to identify the presence of autofluorescent/birefringent gut granules (Laufer et al., 1980). Statistical tests of significance were made using the Student's t-test in Excel and graphs were made using GraphPad Prism Version 6.0.

Immunofluorescence and quantification of staining

All embryos used for PAR-3 staining were from worms grown at 25°C, while embryos stained with other antibodies were from worms grown at 19.5°C from the L3/L4 stage. Worms were dissected in water of the same temperature on slides, frozen in liquid nitrogen, then fixed in methanol at −20°C for 15 min. For P granule staining, a post methanol acetone step was included (Strome and Wood, 1983). Primary antibodies used were monoclonal mouse anti–PAR-3 (Nance et al., 2003), OIC1D4 monoclonal mouse anti-P granule (Strome, 1986), anti-PIE-1 (Tenenhaus et al., 1998) and pY99 (Santa Cruz Biotechnology). Monoclonal antibodies were obtained from the Developmental Studies Hybridoma Bank, University of Iowa. Secondary antibodies included Alexa Fluor 594-labeled goat anti-mouse (Invitrogen) and Cy3-labeled donkey anti-mouse (Jackson ImmunoResearch). Slides were mounted with Vectashield containing DAPI (Vector Laboratories). Images were acquired on a Leica DM RA2 microscope fitted with a Hamamatsu Orca-ER digital Camera using OpenLab software (Improvision).

OpenLab software was used to measure the length of the PAR-3 anterior–posterior domain and overall length of embryos in pixels, which was then converted to %EL. Measurements were taken twice for each embryo. For quantification of pY99 staining, four-cell embryos whose P_2 and EMS were in interphase to metaphase were used. Fluorescence intensities were traced along the EMS-P_2 and EMS-ABp cell-cell contacts using the segmented line tool of the Fiji software. The ratios of EMS-P_2 cortical to the EMS-ABp cortical pixel intensities were then calculated for each embryo, and were averaged for each genotype.

Statistical tests of significance were made using the Student's t-test in Excel and the scatterplot was created in GraphPad Prism Version 6.0.

Supplementary Material

Refer to Web version on PubMed Central for supplementary material.

Acknowledgements:

We thank Gian Garriga, Craig Mello and Susan Strome for strains and Jim Priess's lab for PIE-1 antibody. Some strains were provided by the CGC, which is funded by NIH Office of Research Infrastructure Programs (P40 OD010440). We are grateful to Neil Willits, UC Davis Department of Statistics, for assistance with the Chi-squared analysis. We thank members of the Rose and McNally labs, the UC Davis SuperWorm group, Ken Kemphues, members of the Kemphues lab, and Kelly Liu for helpful discussion. We also thank Ken Kemphues for helpful comments on the manuscript. This work was supported by NIH (R01GM68744) and by NIFA (CA-D* -MCB-6239-H) wards to L.R. and by an NIH (R01GM079112) award to Kenneth Kemphues.

References

Bei Y, Hogan J, Berkowitz LA, Soto M, Rocheleau CE, Pang KM, Collins J, Mello CC, 2002 SRC-1 and Wnt signaling act together to specify endoderm and to control cleavage orientation in early C. elegans embryos. Developmental cell 3, 113–125. [PubMed: 12110172]

Bergstralh DT, Dawney NS, St Johnston D, 2017 Spindle orientation: a question of complex positioning. Development 144, 1137–1145. [PubMed: 28351864]

Berkowitz LA, Strome S, 2000 MES-1, a protein required for unequal divisions of the germline in early C. elegans embryos, resembles receptor tyrosine kinases and is localized to the boundary between the germline and gut cells. Development 127, 4419–4431. [PubMed: 11003841]

Brenner S, 1974 The genetics of Caenorhabditis elegans. Genetics 77, 71–94. [PubMed: 4366476]

Cheeks RJ, Canman JC, Gabriel WN, Meyer N, Strome S, Goldstein B, 2004 C. elegans PAR proteins function by mobilizing and stabilizing asymmetrically localized protein complexes. Current biology : CB 14, 851–862. [PubMed: 15186741]

Church DL, Guan KL, Lambie EJ, 1995 Three genes of the MAP kinase cascade, mek-2, mpk-1/sur-1 and let-60 ras, are required for meiotic cell cycle progression in Caenorhabditis elegans. Development 121, 2525–2535. [PubMed: 7671816]

Cordes S, Frank CA, Garriga G, 2006 The C. elegans MELK ortholog PIG-1 regulates cell size asymmetry and daughter cell fate in asymmetric neuroblast divisions. Development 133, 2747–2756. [PubMed: 16774992]

Cuenca AA, Schetter A, Aceto D, Kemphues K, Seydoux G, 2003 Polarization of the C. elegans zygote proceeds via distinct establishment and maintenance phases. Development 130, 1255–1265. [PubMed: 12588843]

di Pietro F, Echard A, Morin X, 2016 Regulation of mitotic spindle orientation: an integrated view. EMBO Rep 17, 1106–1130. [PubMed: 27432284]

Drewes G, Ebneth A, Preuss U, Mandelkow EM, Mandelkow E, 1997 MARK, a novel family of protein kinases that phosphorylate microtubule-associated proteins and trigger microtubule disruption. Cell 89, 297–308. [PubMed: 9108484]

Etemad-Moghadam B, Guo S, Kemphues KJ, 1995 Asymmetrically distributed PAR-3 protein contributes to cell polarity and spindle alignment in early C. elegans embryos. Cell 83, 743–752. [PubMed: 8521491]

Gil M, Yang Y, Lee Y, Choi I, Ha H, 1997 Cloning and expression of a cDNA encoding a novel protein serine/threonine kinase predominantly expressed in hematopoietic cells. Gene 195, 295–301. [PubMed: 9305775]

Goldstein B, 1993 Establishment of gut fate in the E lineage of C. elegans: the roles of lineage-dependent mechanisms and cell interactions. Development 118, 1267–1277. [PubMed: 8269853]

Goldstein B, 1995a An analysis of the response to gut induction in the C. elegans embryo. Development 121, 1227–1236. [PubMed: 7743934]

Goldstein B, 1995b Cell contacts orient some cell division axes in the Caenorhabditis elegans embryo. The Journal of cell biology 129, 1071–1080. [PubMed: 7744956]

Goldstein B, Macara IG, 2007 The PAR proteins: fundamental players in animal cell polarization. Developmental cell 13, 609–622. [PubMed: 17981131]

Heyer BS, Warsowe J, Solter D, Knowles BB, Ackerman SL, 1997 New member of the Snf1/AMPK kinase family, Melk, is expressed in the mouse egg and preimplantation embryo. Mol Reprod Dev 47, 148–156. [PubMed: 9136115]

Hurd DD, Kemphues KJ, 2003 PAR-1 is required for morphogenesis of the Caenorhabditis elegans vulva. Developmental biology 253, 54–65. [PubMed: 12490197]

Kamath RS, Fraser AG, Dong Y, Poulin G, Durbin R, Gotta M, Kanapin A, Le Bot N, Moreno S, Sohrmann M, Welchman DP, Zipperlen P, Ahringer J, 2003 Systematic functional analysis of the Caenorhabditis elegans genome using RNAi. Nature 421, 231–237. [PubMed: 12529635]

Kemphues KJ, Priess JR, Morton DG, Cheng NS, 1988 Identification of genes required for cytoplasmic localization in early C. elegans embryos. Cell 52, 311–320. [PubMed: 3345562]

Kirby C, Kusch M, Kemphues K, 1990 Mutations in the par genes of Caenorhabditis elegans affect cytoplasmic reorganization during the first cell cycle. Developmental biology 142, 203–215. [PubMed: 2227096]

Krueger LE, Wu JC, Tsou MF, Rose LS, 2010 LET-99 inhibits lateral posterior pulling forces during asymmetric spindle elongation in C. elegans embryos. The Journal of cell biology 189, 481–495. [PubMed: 20421425]

Laufer JS, Bazzicalupo P, Wood WB, 1980 Segregation of developmental potential in early embryos of Caenorhabditis elegans. Cell 19, 569–577. [PubMed: 7363324]

Lin A, Giuliano CJ, Sayles NM, Sheltzer JM, 2017 CRISPR/Cas9 mutagenesis invalidates a putative cancer dependency targeted in on-going clinical trials. Elife 6.

Liro MJ, Rose LS, 2016 Mitotic Spindle Positioning in the EMS Cell of Caenorhabditis elegans Requires LET-99 and LIN-5/NuMA. Genetics.

Liu J, Maduzia LL, Shirayama M, Mello CC, 2010 NMY-2 maintains cellular asymmetry and cell boundaries, and promotes a SRC-dependent asymmetric cell division. Developmental biology 339, 366–373. [PubMed: 20059995]

Maduro MF, 2017 Gut development in C. elegans. Seminars in cell & developmental biology.

Mello CC, Schubert C, Draper B, Zhang W, Lobel R, Priess JR, 1996 The PIE-1 protein and germline specification in C. elegans embryos. Nature 382, 710–712. [PubMed: 8751440]

Morton DG, Hoose WA, Kemphues KJ, 2012 A genome-wide RNAi screen for enhancers of par mutants reveals new contributors to early embryonic polarity in Caenorhabditis elegans. Genetics 192, 929–942. [PubMed: 22887819]

Motegi F, Zonies S, Hao Y, Cuenca AA, Griffin E, Seydoux G, 2011 Microtubules induce self-organization of polarized PAR domains in Caenorhabditis elegans zygotes. Nature cell biology 13, 1361–1367. [PubMed: 21983565]

Munro E, Nance J, Priess JR, 2004 Cortical flows powered by asymmetrical contraction transport PAR proteins to establish and maintain anterior-posterior polarity in the early C. elegans embryo. Developmental cell 7, 413–424. [PubMed: 15363415]

Nakano I, Paucar AA, Bajpai R, Dougherty JD, Zewail A, Kelly TK, Kim KJ, Ou J, Groszer M, Imura T, Freije WA, Nelson SF, Sofroniew MV, Wu H, Liu X, Terskikh AV, Geschwind DH, Kornblum HI, 2005 Maternal embryonic leucine zipper kinase (MELK) regulates multipotent neural progenitor proliferation. The Journal of cell biology 170, 413427.

Nance J, Munro EM, Priess JR, 2003 C. elegans PAR-3 and PAR-6 are required for apicobasal asymmetries associated with cell adhesion and gastrulation. Development 130, 5339–5350. [PubMed: 13129846]

Nance J, Priess JR, 2002 Cell polarity and gastrulation in C. elegans. Development 129, 387–397. [PubMed: 11807031]

Neumuller RA, Knoblich JA, 2009 Dividing cellular asymmetry: asymmetric cell division and its implications for stem cells and cancer. Genes & development 23, 2675–2699. [PubMed: 19952104]

Offenburger SL, Bensaddek D, Murillo AB, Lamond AI, Gartner A, 2017 Comparative genetic, proteomic and phosphoproteomic analysis of C. elegans embryos with a focus on ham-1/STOX and pig-1/MELK in dopaminergic neuron development. Sci Rep 7, 4314. [PubMed: 28659600]

Pacquelet A, Uhart P, Tassan JP, Michaux G, 2015 PAR-4 and anillin regulate myosin to coordinate spindle and furrow position during asymmetric division. The Journal of cell biology 210, 1085–1099. [PubMed: 26416962]

Park DH, Rose LS, 2008 Dynamic localization of LIN-5 and GPR-1/2 to cortical force generation domains during spindle positioning. Developmental biology 315, 42–54. [PubMed: 18234174]

Praitis V, Casey E, Collar D, Austin J, 2001 Creation of low-copy integrated transgenic lines in Caenorhabditis elegans. Genetics 157, 1217–1226. [PubMed: 11238406]

Rose L, Gonczy P, 2014 Polarity establishment, asymmetric division and segregation of fate determinants in early C. elegans embryos. WormBook : the online review of C. elegans biology, 1–43.

Rose LS, Kemphues K, 1998 The let-99 gene is required for proper spindle orientation during cleavage of the C. elegans embryo. Development 125, 1337–1346. [PubMed: 9477332]

Sailer A, Anneken A, Li Y, Lee S, Munro E, 2015 Dynamic Opposition of Clustered Proteins Stabilizes Cortical Polarity in the C. elegans Zygote. Developmental cell 35, 131–142. [PubMed: 26460948]

Schindelin J, Arganda-Carreras I, Frise E, Kaynig V, Longair M, Pietzsch T, Preibisch S, Rueden C, Saalfeld S, Schmid B, Tinevez JY, White DJ, Hartenstein V, Eliceiri K, Tomancak P, Cardona A, 2012 Fiji: an open-source platform for biological-image analysis. Nature methods 9, 676–682. [PubMed: 22743772]

Schlesinger A, Shelton CA, Maloof JN, Meneghini M, Bowerman B, 1999 Wnt pathway components orient a mitotic spindle in the early Caenorhabditis elegans embryo without requiring gene transcription in the responding cell. Genes & development 13, 2028–2038. [PubMed: 10444600]

Schubert CM, Lin R, de Vries CJ, Plasterk RH, Priess JR, 2000 MEX-5 and MEX-6 function to establish soma/germline asymmetry in early C. elegans embryos. Molecular cell 5, 671–682. [PubMed: 10882103]

Small LE, Dawes AT, 2017 PAR proteins regulate maintenance-phase myosin dynamics during Caenorhabditis elegans zygote polarization. Molecular biology of the cell 28, 2220–2231. [PubMed: 28615321]

Spilker AC, Rabilotta A, Zbinden C, Labbe JC, Gotta M, 2009 MAP kinase signaling antagonizes PAR-1 function during polarization of the early Caenorhabditis elegans embryo. Genetics 183, 965–977. [PubMed: 19720857]

Strome S, 1986 Asymmetric movements of cytoplasmic components in Caenorhabditis elegans zygotes. J Embryol Exp Morphol 97 Suppl, 15–29. [PubMed: 3625110]

Strome S, Wood WB, 1982 Immunofluorescence visualization of germ-line-specific cytoplasmic granules in embryos, larvae, and adults of Caenorhabditis elegans. Proceedings of the National Academy of Sciences of the United States of America 79, 1558–1562. [PubMed: 7041123]

Strome S, Wood WB, 1983 Generation of asymmetry and segregation of germ-line granules in early C. elegans embryos. Cell 35, 15–25. [PubMed: 6684994]

Sumiyoshi E, Takahashi S, Obata H, Sugimoto A, Kohara Y, 2011 The beta-catenin HMP2 functions downstream of Src in parallel with the Wnt pathway in early embryogenesis of *C. elegans*. Developmental biology 355, 302–312. [PubMed: 21575624]

Tenenhaus C, Schubert C, Seydoux G, 1998 Genetic requirements for PIE-1 localization and inhibition of gene expression in the embryonic germ lineage of Caenorhabditis elegans. Developmental biology 200, 212–224. [PubMed: 9705228]

Timmons L, Fire A, 1998 Specific interference by ingested dsRNA. Nature 395, 854. [PubMed: 9804418]

Tsou MF, Hayashi A, DeBella LR, McGrath G, Rose LS, 2002 LET-99 determines spindle position and is asymmetrically enriched in response to PAR polarity cues in C. elegans embryos. Development 129, 4469–4481. [PubMed: 12223405]

Wang Y, Lee YM, Baitsch L, Huang A, Xiang Y, Tong H, Lako A, Von T, Choi C, Lim E, Min J, Li L, Stegmeier F, Schlegel R, Eck MJ, Gray NS, Mitchison TJ, Zhao JJ, 2014 MELK is an oncogenic kinase essential for mitotic progression in basal-like breast cancer cells. Elife 3, e01763. [PubMed: 24844244]

Wei H, Yan B, Gagneur J, Conradt B, 2017 Caenorhabditis elegans CES-1 Snail Represses pig-1 MELK Expression To Control Asymmetric Cell Division. Genetics 206, 2069–2084. [PubMed: 28652378]

Wu JC, Rose LS, 2007 PAR-3 and PAR-1 inhibit LET-99 localization to generate a cortical band important for spindle positioning in Caenorhabditis elegans embryos. Molecular biology of the cell 18, 4470–4482. [PubMed: 17761536]

Wu Y, Griffin EE, 2017 Regulation of Cell Polarity by PAR-1/MARK Kinase. Curr Top Dev Biol 123, 365–397. [PubMed: 28236972]

Zonies S, Motegi F, Hao Y, Seydoux G, 2010 Symmetry breaking and polarization of the C. elegans zygote by the polarity protein PAR-2. Development 137, 1669–1677. [PubMed: 20392744]

Highlights

- PIG-1 kinase acts redundantly with PAR-1 kinase in early *C. elegans* development.
- PIG-1 and PAR-1 prevent expansion of the PAR-3 domain in the one-cell embryo
- PIG-1 and PAR-1 regulate spindle orientation in the EMS cell at the four-cell stage
- PIG-1 acts in the MES-1/SRC-1 pathway for spindle positioning

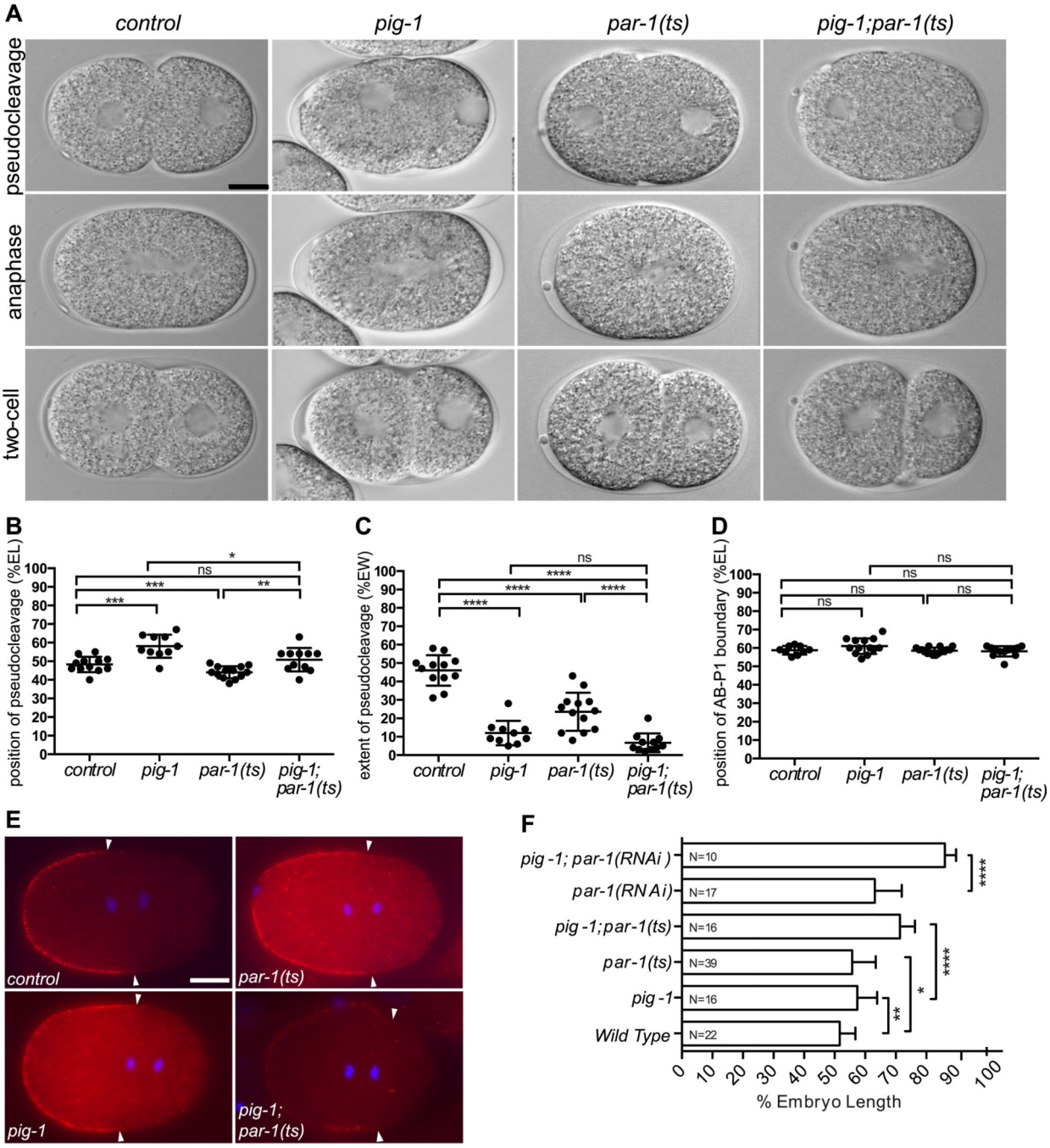

Figure 1. *pig-1* mutants exhibit reduced contractility and expansion of the PAR-3 domain.

(A) Images from time-lapse microscopy of control (wild type), *pig-1(gm344) GFP::tubulin, par-1(zu310ts)* and *pig-1(gm344);par-1(zu310ts)* embryos grown and imaged at 25°C. Anterior is to the left and posterior to the right in this and all embryo images. Scale bar: 10μm. (B-D) Quantification of phenotypes of the same genotypes as in (A) except that *GFP::tubulin* embryos were used as controls. (B) The position of the pseudocleavage furrow expressed as percent embryo length (%EL), where anterior is 0% and posterior 100% (C) The extent of pseudocleavage furrow ingression, expressed as percentage of embryo width

(%EW). (D) Measurement of the position of the cleavage furrow between P_1 and AB at the early two-cell stage, expressed as %EL. (E) Representative images of one-cell embryos at anaphase showing anti-PAR-3 antibody staining (red) in control (wild type), *pig-1(gm344)*, *par-1(zu310ts)*, and *pig-1(gm344);par-1(zu310ts)* embryos grown at 25°C. Arrowheads mark the extent of the PAR-3 domain. DAPI (blue) marks the DNA. Scale bar: 10μm. (F) Quantification of the posterior boundary of the cortical PAR-3 domain, expressed as %EL. Data were compared using the unpaired Student's t-test and statistical values shown as: ns (not significant), $P > 0.05$; *, $P \leq 0.05$; **, $P \leq 0.01$; ***, $P \leq 0.001$; ****, $P \leq 0.0001$; see Table S2 for specific P values.

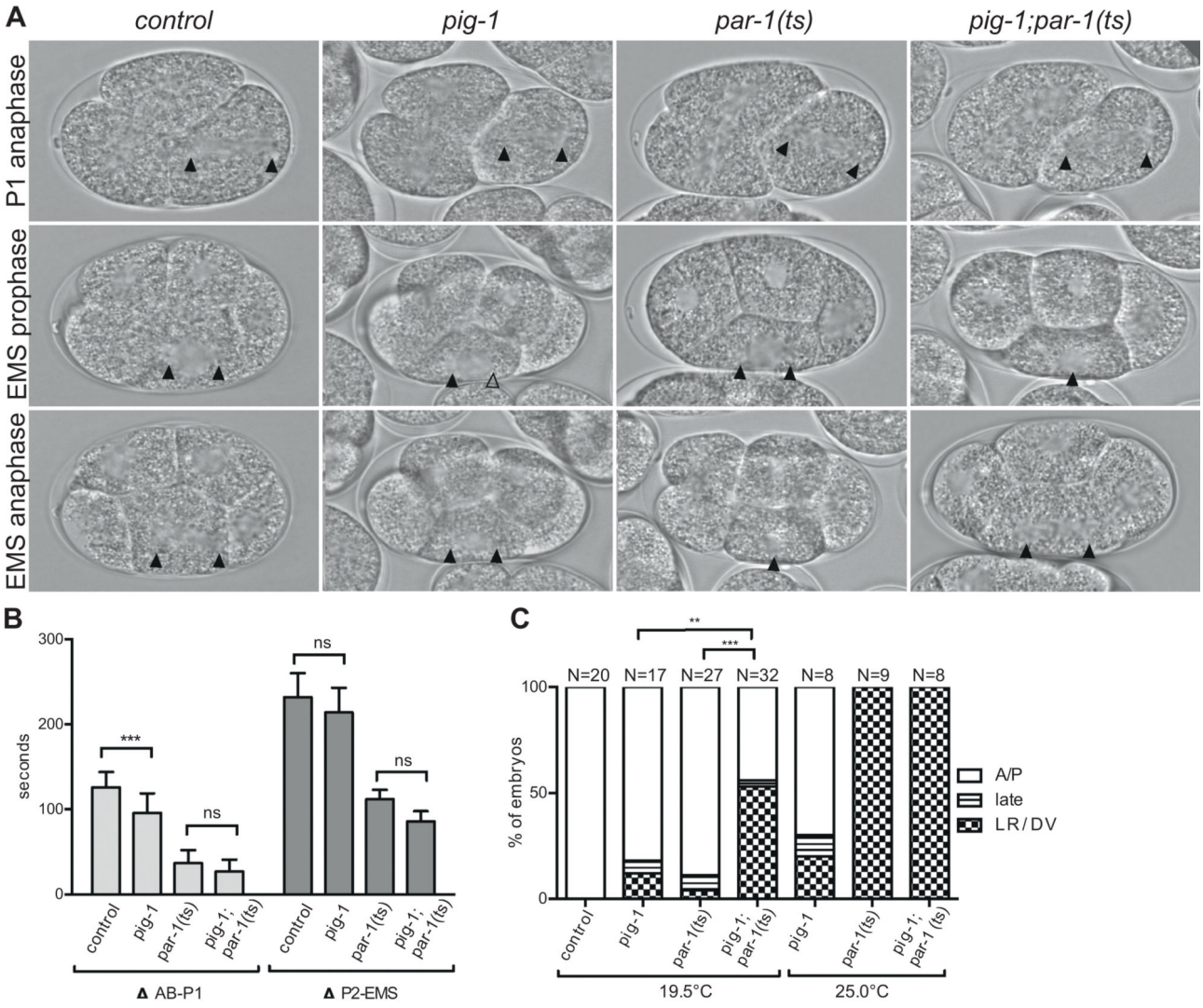

Figure 2. Comparison of *pig-1* to *pig-1;par-1* double mutant embryos.

Data for A and B were obtained from control (wild type), *pig-1(gm344) GFP::tubulin, par-1(zu310ts)* and *pig-1(gm344);par-1(zu310ts)* embryos grown and imaged at 19.5 °C. (A) Images from time-lapse microscopy. Closed arrowheads point to centrosomes in focus and the open arrowhead points to a centrosome that was slightly out of the focal plane in that frame. (B) Cell cycle comparison between indicated genotypes. The difference between the time of onset of nuclear envelope breakdown for AB-P_1 and EMS- P_2 sister cells is shown on the y-axis. Data were compared using the unpaired Student's t-test. (C) Quantification of spindle positioning at the indicated temperatures; *GFP::tubulin* embryos were used as controls. The AP category includes embryos whose centrosomes were aligned on the AP axis before nuclear envelope breakdown. The late rotation category refers to EMS spindle alignment with the AP axis that occurred after NEB; the LR/DV category includes final spindle positions on all non-AP axes. The proportion of normal (AP) and abnormal (late and LR/DV) embryos were compared between genotypes using Chisquared analysis. For both B and C statistical values are shown as: ns (not significant), $P > 0.05$; *, $P \leq 0.05$; **, $P \leq 0.01$; ***, $P \leq 0.001$; ****, $P \leq 0.0001$; see Table S2 for specific P values.

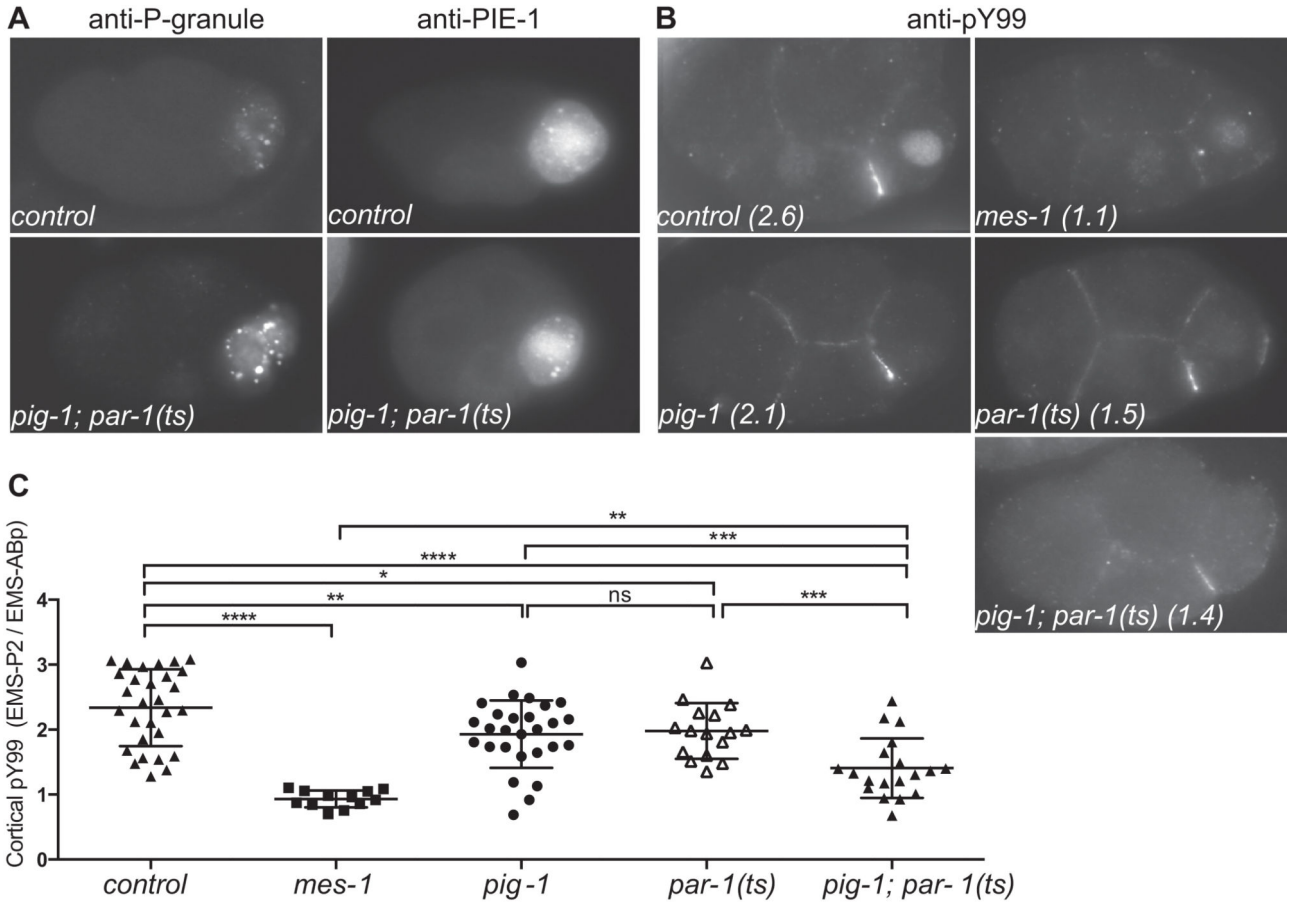

Figure 3. Analysis of cell fate markers in *pig-1* and *par-1* mutants.

(A) Representative images of P-granule and PIE-1 localization in control (wild type), and *pig-1(gm344);par-1(310ts)* double mutant embryos. (B) Anti-phosphotyrosine antibody staining in control (wild type), *mes-1(bn74)*, *pig-1(gm344), par-1(zu310ts)* and *pig-1(gm344);par-1(zu310ts)* embryos at 19.5°C. Embryos were in prophase or prometaphase of the EMS cell cycle. Values in parentheses refer to the ratio of the pY99 signal at the EMS-P_2 cortex over the EMS-ABp cortical signal for the specific image shown. (C) Scatterplot of the ratio of pY99 signals at the EMS-P_2 cell-cell contact site over EMS-ABp contact site for individual embryos of each genotype indicated. The anti-pY99 antibody also stains nuclei in a SRC dependent manner, as reported in (Sumiyoshi et al., 2011). Data were compared using the unpaired Student's t-test: ns (not significant), $P > 0.05$; *, $P \leq 0.05$; **, $P \leq 0.01$; ***, $P \leq 0.001$; ****, $P \leq 0.0001$; see Table S2 for specific P values.

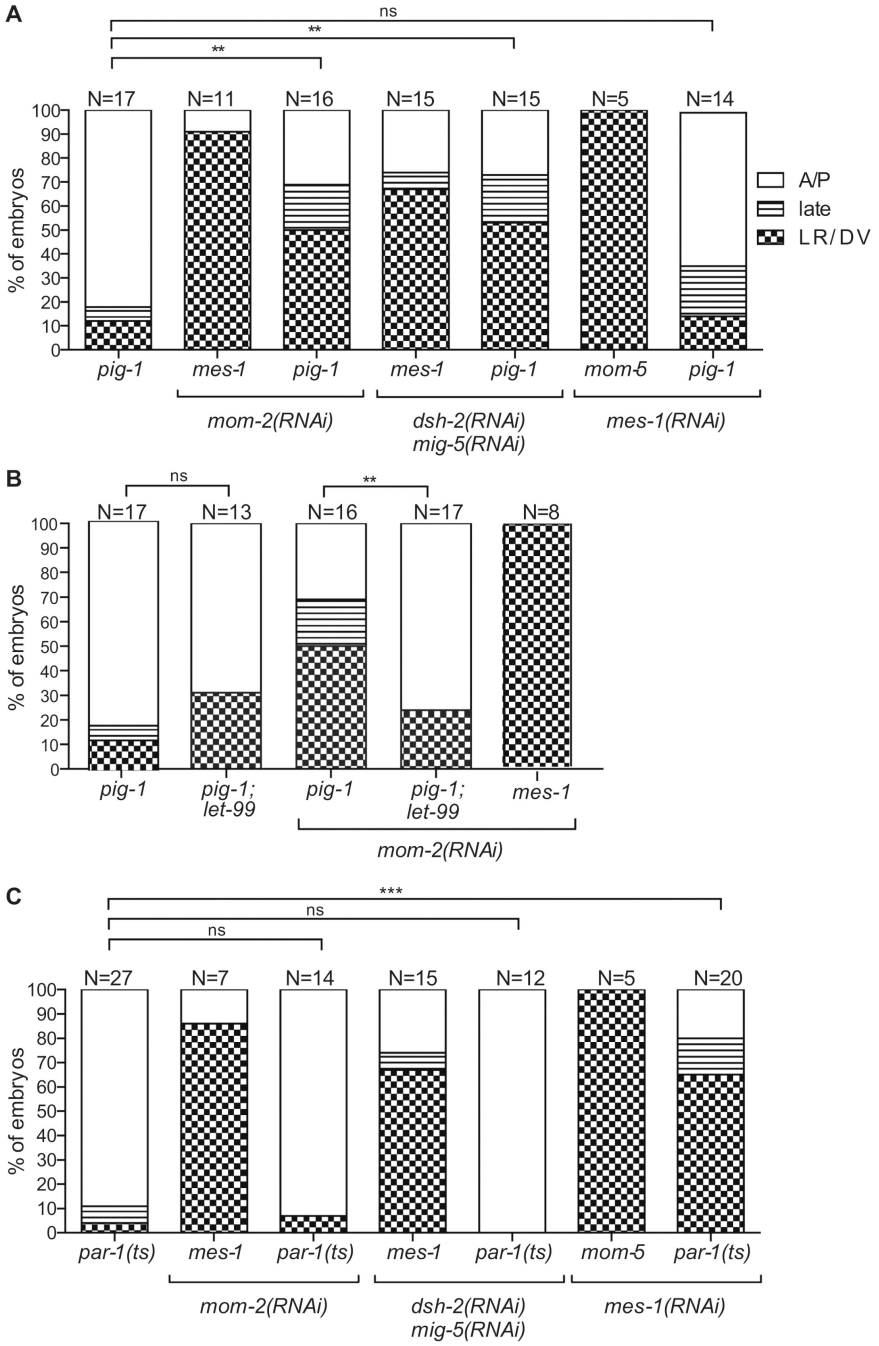

Figure 4. PIG-1 acts in the MES-1/SRC-1 pathway and PAR-1 acts in the Wnt pathway for EMS spindle positioning.

(A) Quantification of EMS spindle positioning in embryos grown at the semi-permissive temperature of 19.5°C (A and C) or embryos grown at 16°C and upshifted to 25°C at the four- cell stage (B). Spindle orientation was scored as in Fig. 2. *GFP::tubulin* embryos were used as controls. Additional control RNAi treatments were carried out in parallel: *mom-2(RNAi)* exhibited 21/21 AP divisions, *dsh-2(RNAi); mig-5(RNAi)* embryos exhibited 9/9 AP divisions, and *mes-1(RNAi)* embryos exhibited 7/8 AP divisions and 1/8 late

rotation. Data were compared using Chi-squared analysis: ns (not significant), $P > 0.05$; *, $P \leq 0.05$; **, $P \leq 0.01$; ***, $P \leq 0.001$; ****, $P \leq 0.0001$; see Table S2 for specific P values.

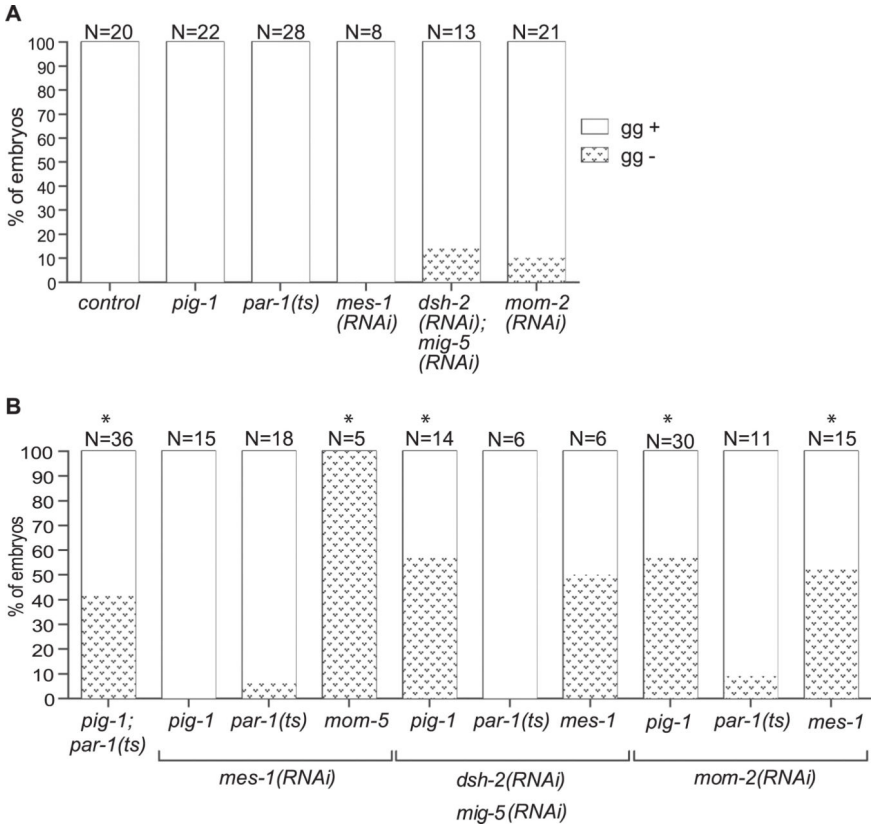

Figure 5. PIG-1 acts in the MES-1 pathway for endoderm specification.

Quantification of the presence (gg+) or absence (gg-) of gut granules, as a marker for endoderm differentiation, performed on embryos raised at 19.5°C. (A) *pig-1(gm344), par-1(zu310ts), mes-1(RNAi), dsh-2(RNAi);mig-5(RNAi),* and *mom-2(RNAi)* single mutants and (B) double mutant combinations. *GFP::tubulin* embryos were used as controls. Data were compared using Chi-squared analysis. None of the single mutants in (A) were statistically different from control; in (B) an * signifies that a given double mutant was statistically different from one or both single mutants. See Table S2 for specific P values.